**The EMBO Journal** Vol.17 No.18 pp.5458–5465, 1998

# Structure of the double-stranded RNA-binding domain of the protein kinase PKR reveals the molecular basis of its dsRNA-mediated activation

**Sambasivarao Nanduri, Bruce W.Carpick[1], Yanwu Yang, Bryan R.G.Williams[1] and Jun Qin[2]**

Structural Biology Program and [1]Department of Cancer Biology, Lerner Research Institute, The Cleveland Clinic Foundation, 9500 Euclid Avenue, Cleveland, OH 44195, USA

[2]Corresponding author
e-mail: qinj@cesmtp.ccf.org

**Protein kinase PKR is an interferon-induced enzyme that plays a key role in the control of viral infections and cellular homeostasis. Compared with other known kinases, PKR is activated by a distinct mechanism that involves double-stranded RNA (dsRNA) binding in its N-terminal region in an RNA sequence-independent fashion. We report here the solution structure of the 20 kDa dsRNA-binding domain (dsRBD) of human PKR, which provides the first three-dimensional insight into the mechanism of its dsRNA-mediated activation. The structure of dsRBD exhibits a dumb-bell shape comprising two tandem linked dsRNA-binding motifs (dsRBMs) both with an α-β-β-β-α fold. The structure, combined with previous mutational and biochemical data, reveals a highly conserved RNA-binding site on each dsRBM and suggests a novel mode of protein–RNA recognition. The central linker is highly flexible, which may enable the two dsRBMs to wrap around the RNA duplex for cooperative and high-affinity binding, leading to the overall change of PKR conformation and its activation.**

*Keywords*: dsRNA-binding domain/NMR/PKR/solution structure

## Introduction

One of the earliest cellular responses during viral infections is the production of interferon that in turn induces antiviral proteins. The protein kinase PKR is a key component of the host defense system that is induced by interferon (Meurs *et al*., 1990; Koromilas *et al*., 1992; Maran *et al*., 1994; Williams, 1995; Clemens, 1997). PKR is known to function in the cellular antiviral response (Samuel *et al*., 1984; Rice *et al*., 1985) through inhibition of eukaryotic initiation factor 2 (eIF-2) via phosphorylation of serine and threonine residues on its α-subunit (Chong *et al*., 1992). More recently, PKR has been shown to activate several transcription factors including NF-κB and IRF-1 in response to different extracellular stimuli (Kumar *et al*., 1994, 1997; Maran *et al*., 1994; Beretta *et al*., 1996). A growing amount of evidence indicates that PKR is involved in normal control of cell growth, differentiation and apoptosis and acts as a signal transducer at both the transcriptional and translational levels (Maran *et al*., 1994; Donze *et al*., 1995; Wu and Kaufman, 1996; Brand *et al*., 1997; Der *et al*., 1997; Wong *et al*., 1997; Zhu *et al*., 1997).

A unique and critical step in the activation of PKR, compared with other kinases, is the specific interaction of its N-terminal double-standed RNA-binding domain (dsRBD) with double-stranded RNA (dsRNA) in an RNA sequence-independent manner (Figure 1A). Upon binding to dsRNA, PKR is thought to undergo conformational rearrangement and autophosphorylation, which leads to the phosphorylation of eIF-2 (Chong *et al*., 1992) and other target proteins (Galabru and Hovanessian, 1985; Kumar *et al*., 1994; Brand *et al*., 1997). The dsRBD comprises two tandem copies of a 65–68 amino acid dsRNA-binding motif (dsRBM) (Figure 1A and B) that has been identified in >20 functionally distinct RNA-binding proteins (Kharrat *et al*., 1995). dsRBM1 in PKR appears to be more important in dsRNA binding (Green and Mathews, 1992; Schmedt *et al*., 1995) and matches the dsRBM consensus sequence more closely than does dsRBM2 (Figure 1B), whereas both motifs are indispensable for the specific and high affinity dsRNA binding in the regulation of PKR function, as shown by deletional and mutational analyses (Patel and Sen, 1992; Bevilacqua and Cech, 1996; Patel *et al*., 1996). While the interaction of dsRNA with the dsRBD is sequence independent (Hunter *et al*., 1975; Minks *et al*., 1979; Manche *et al*., 1992), the recognition mechanism appears to be novel, involving minor groove interactions of a network of 2′-OHs of the RNA duplex with dsRBD (Bevilacqua and Cech, 1996). Despite the extensive mutational and biochemical studies, the detailed molecular basis of how dsRBD modulates PKR activity by binding to dsRNA remains elusive. Here we report the solution structure of the 20 kDa dsRBD determined by multidimensional heteronuclear NMR. Combined with previous mutational and biochemical data, this structure provides the first three-dimensional insight into the mechanism of dsRBD–dsRNA interaction and subsequent PKR activation.

## Results and discussion

### *Overall structure of dsRBD*

The structure of dsRBD exhibits a dumb-bell shape, with the two dsRBMs flanking a 22 residue linker region (Figure 2A). Both dsRBMs in the structure are well defined except for the N-terminal residues 1–9 for dsRBM1 and 169–174 for dsRBM2 (Figure 2B; Table I). Each dsRBM contains an α-β-β-β-α fold in which the two helices lie on one side and pack against a three-stranded antiparallel β-sheet (Figure 2A). The linker between the two dsRBMs was found to be long and highly flexible, as shown by the random chemical shift nature, small and negative heteronuclear amide $^{1}H\{^{15}N\}$ nuclear Overhauser effects (NOEs) in this region (Figure 3). In fact, no

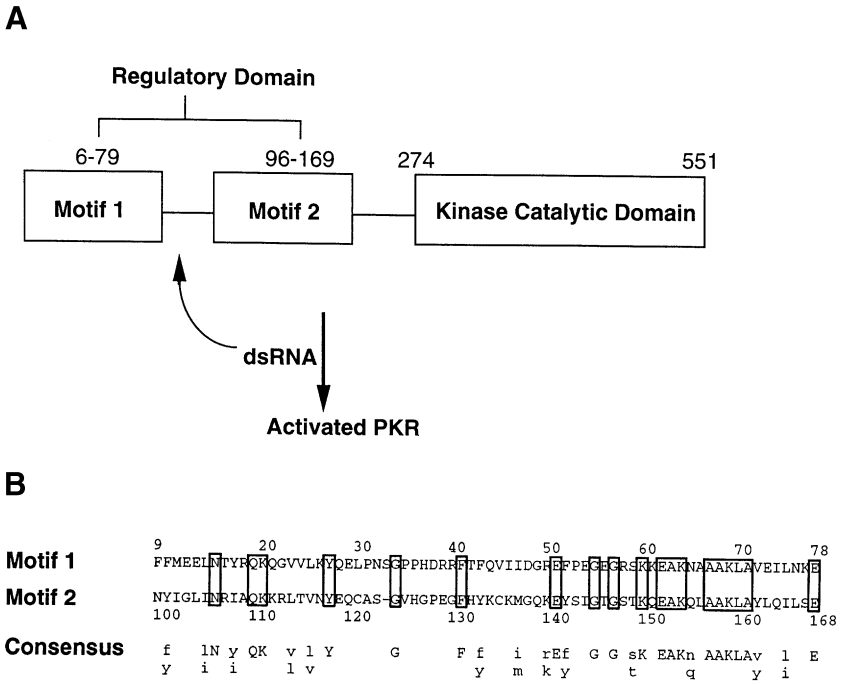


**Fig. 1.** Schematic representation of PKR showing its primary structure and sequence alignment for the dsRBMs. (**A**) The N-terminal regulatory domain and the C-terminal catalytic (kinase) domain. dsRNA binds to the regulatory domain and induces PKR activation. The positions of the two dsRNA-binding motifs within the regulatory domain are indicated. (**B**) Amino acid sequence alignment of dsRBM1 and dsRBM2 of human PKR. Identical residues within the two motifs are boxed. The consensus sequence of dsRBM is shown, with identical residues listed in upper case and similar residues in lower case. The amino acids are identified by their one-letter codes.

long-range NOEs and few medium-range NOEs were identified in this region due to its high flexibility. Although dsRBD is in a monomeric form as shown by its overall correlation time (~9.1 ns) and gel filtration experiments (Nanduri *et al*., 1998), its size is relatively large (20 kDa) for NMR structure determination, particularly because some repeated sequences of the two dsRBMs increased the degree of chemical shift degeneracy. This necessitated 20 three-dimensional and four-dimensional double and triple resonance experiments for complete resonance assignment (Nanduri *et al*., 1998) and NOE analysis. Among these experiments, 4D $^{13}C/^{15}N$-edited NOESY and 4D $^{13}C/^{13}C$ NOESY were especially valuable for the unambiguous assignment of medium and long-range NOEs. Table I lists the final structural constraints and statistics that demonstrate the good quality of the calculated structure.

### *Structural similarities of dsRBMs in PKR and other dsRNA-binding proteins*

With ~50% sequence homology (27% sequence identity) that occurs strongly in the C-terminus of the dsRBMs (Figure 1B), the two motifs exhibit very similar tertiary folds with a backbone r.m.s.d. of 2 Å (Figure 4). A central hydrophobic core appears to play a critical role in stabilizing this conserved fold for each dsRBM, which involves highly conserved hydrophobic residues such as F10, F43, V45, I47, A71 and V72 for dsRBM1, and Y101, Y133, C135, M137 and A161 for dsRBM2. Particular attention was paid during the NOE analysis to see if there were any inter-domain contacts between dsRBM1 and dsRBM2, and no such contacts were found. The folding topology of each dsRBM in PKR is similar to the recently reported dsRBM structures from *Escherichia coli* RNase III and *Drosophila* Staufen protein, respectively (Figure 4) (Bycroft *et al*., 1995; Kharrat *et al*., 1995). The backbone r.m.s.ds between each dsRBM of PKR and Staufen dsRBM are 2.3 and 2.2 Å, respectively (~23% sequence identity between each dsRBM and Staufen dsRBM). The copy numbers of dsRBMs for different dsRNA-binding proteins vary extensively (Kharrat *et al*., 1995). The multiple copies of dsRBMs may form specific recognition patterns, leading to different specificities and affinities for dsRNA. In the case of PKR, although dsRBM1 appears to have higher dsRNA binding affinity than dsRBM2 (Green and Mathews, 1992; Schmedt *et al*., 1995), both dsRBMs are important for the high affinity dsRNA binding and subsequent PKR activation (Patel and Sen, 1992; Schmedt *et al*., 1995; Bevilacqua and Cech, 1996; Patel *et al*., 1996). The two dsRBMs linked by the long and flexible loop in PKR may bind to dsRNA in a cooperative fashion (see below), consistent with the biochemical and biophysical analyses (Schmedt *et al*., 1995; Bevilacqua and Cech, 1996; Carpick *et al*., 1997).

### *Correlation of the structure with mutational effects and identification of dsRNA-binding sites*

Extensive mutational studies have been performed previously on PKR and were aimed at pinpointing the critical residues for RNA binding (Clarke and Mathews, 1995; McMillan *et al*., 1995; Patel *et al*., 1996). Analysis of the surface residues using data from these mutational studies reveals a highly conserved RNA-binding site on each dsRBM. For dsRBM1, R39, F41, S59, K60, K61 and K64 form a cluster of surface residues where point mutations either severely decrease or completely abolish the dsRNA binding (Clarke and Mathews, 1995; McMillan *et al*., 1995; Patel *et al*., 1996), suggesting a positively charged

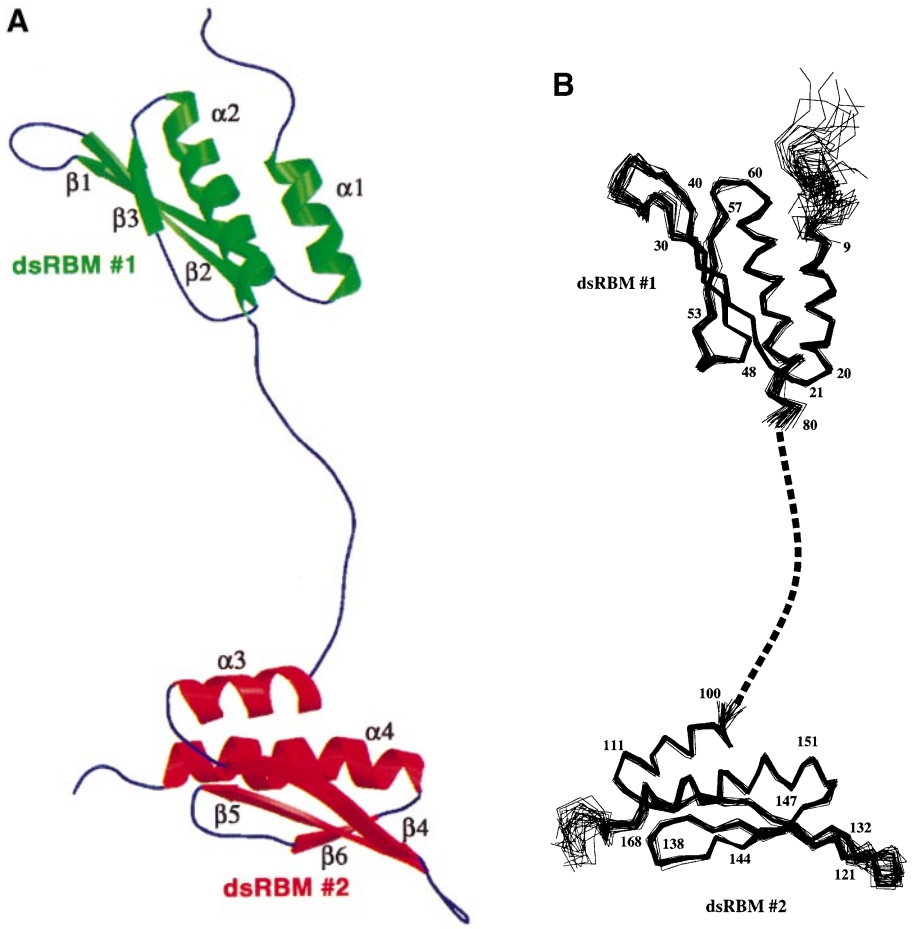


**Fig. 2.** Illustration of dsRBD structure. (**A**) Ribbon representation of dsRBD containing dsRBM1 (green) and dsRBM2 (red) linked by a 22 amino acid loop. The secondary structural elements are labeled sequentially as α1, α2, α3 and α4 for α-helices, and β1, β2, β3, β4, β5, β6, β7 and β8 for β-sheets respectively. The figure was prepared using the program MOLSCRIPT (Kraulis, 1991). (**B**) Backbone superpositions of 30 simulated annealing structures of dsRBM1 and dsRBM2. For clarity, the linker which is highly flexible and has a high r.m.s.d. (3.6 Å for the backbone) is shown by a dashed line (see text). The statistics of the structures are listed in Table I.

binding interface. The surface encompasses the residues from the beginning of β3, the loop between β3 and α2, and the N-terminal part of α2 (Figure 4). While F41 is partially involved in the edge of the hydrophobic core, its aromatic ring points out directly to the surface for potential interaction with RNA duplex (Figure 4). For dsRBM2, mutations of the conserved F131, K150 and K154 also abolish the dsRNA binding of PKR (Patel *et al*., 1996), which indicates a similar RNA-binding site to that of dsRBM1 (Figure 4). The dsRNA-binding site appears to be highly conserved in the dsRBMs and has also been suggested in other dsRNA-binding proteins such as *E.coli* RNase III and *Drosophila* Staufen protein (Bycroft *et al*., 1995; Kharrat *et al*., 1995) (Figure 4).

The structure of dsRBD also explains other deleterious mutations (Green and Mathews, 1992; Patel *et al*., 1994; McMillan *et al*., 1995). These mutations appear to significantly perturb the tertiary structure of the dsRBD and hence affect its dsRNA binding. For example, deletions of regions 1–24, 39–50 and 58–69 all remove important structural elements such as an α-helix or β-strand, and completely abolish the dsRNA binding; R18 and Q19 are located at the end of helix α1 and their point mutations to hydrophobic residues destabilize the helix structure; G57 makes a tight turn between β3 and α2, and hence its mutation into Ala introduces a steric clash; A68D, L75A and A158D mutations are defective because they all destabilize the hydrophobic cores of dsRBM1 and dsRBM2, respectively.

### *Implications of dsRNA–dsRBD interaction and subsequent PKR activation*

The details of dsRBD structure and the identification of its RNA-binding sites provide a structural basis for understanding dsRNA-regulated PKR activation. Assuming that the flexible linker was straight, the distance between the RNA-binding sites of the two dsRBMs would allow PKR to bind as much as 30–33 bp of dsRNA; however, extensive biochemical experiments by Bevilacqua and Cech (1996) have shown that 16 bp of dsRNA is sufficient for the stable binding and that the dsRBD only occupies an 11 bp segment. Moreover, each dsRBM saturates only about half of the 11 bp (Schmedt *et al*., 1995). These results suggest that the two dsRBMs may wrap around the RNA duplex. The wrapped-up binding is known to occur in zinc finger–DNA interaction such as the Zif268–DNA complex which involves multiple flexibly linked zinc fingers bound to the DNA major groove (Palvetich and Pabo, 1991). The RNA-binding surface on each dsRBM including the aromatic residue

**Table I.** Structural statistics for dsRBD of PKR[a]

| | <SA> | $(\overline{SA})$r |
|---|---|---|
| r.m.s.d. from experimental distance restraints (Å) | | |
| all (2580) | 0.066 ± 0.002 | 0.061 |
| sequential ($\|i - j\| = 1$) (716) | 0.071 ± 0.002 | 0.065 |
| medium ($1 < \|i - j\| \leq 5$) (389) | 0.079 ± 0.005 | 0.065 |
| long-range ($\|i - j\| > 5$) (311) | 0.050 ± 0.002 | 0.040 |
| intraresidue (1164) | 0.062 ± 0.002 | 0.054 |
| H-bonds (146) | 0.080 ± 0.011 | 0.069 |
| r.m.s.d. from experimental dihedral restraints (°) (164) | 0.41 ± 0.11 | 0.64 |
| r.m.s.d. from experimental $^3J_{HN\alpha}$ coupling contants (Hz) (139) | 0.77 ± 0.03 | 0.74 |
| r.m.s.d. from from experimental $^{13}C$ shifts | | |
| $^{13}C_\alpha$ (p.p.m.) (175) | 0.93 ± 0.06 | 0.93 |
| $^{13}C_\beta$ (p.p.m.) (157) | 1.15 ± 0.03 | 1.15 |
| r.m.s.d. from idealized covalent geometry | | |
| bonds (Å) | 0.005 ± 0.001 | 0.004 |
| angles (°) | 0.75 ± 0.03 | 0.67 |
| impropers (°) | 0.45 ± 0.03 | 0.56 |
| $E_{L-J}$ (kcal/mol)[b] | –487 ± 27.0 | –361 |
| PROCHECK (Ramachandran plot) | | |
| Most favored regions (%)(10–80 and 100–170) | 71.2 ± 1.9 | 72.9 |
| Additionally and generously allowed regions (%) | 28.6 ± 2.1 | 27.1 |
| Disallowed regions (%) | 0.2 ± 0.4 | 0.0 |
| Coodinate precision[c] | | |
| r.m.s.d. of backbone between <SA> and $(\overline{SA})$r (10–80) (Å) | 0.56 ± 0.12 | |
| r.m.s.d. of backbone between <SA> and $(\overline{SA})$r (100–170) (Å) | 0.67 ± 0.12 | |
| r.m.s.d. of heavy atoms between <SA> and $(\overline{SA})$r (10–80) (Å) | 1.08 ± 0.11 | |
| r.m.s.d. of heavy atoms between <SA> and $(\overline{SA})$r (100–170) (Å) | 1.13 ± 0.12 | |

[a]<SA> indicates the ensemble of the 30 final simulated annealing structures, (SA) the mean structure obtained by averaging the coordinates of the individual SA structures best fitted to each other, and $(\overline{SA})$r is the restrained minimized mean structure obtained by restrained regularization of the mean structure SA.
[b]$E_{L-J}$ is the Lennard–Jones van der Waals energy value calculated with the CHARMM empirical energy function and is not included in the target function for SA or restrained minimization.
[c]10–80 and 100–170 regions correspond to the well-defined dsRBM1 and dsRBM2, respectively.

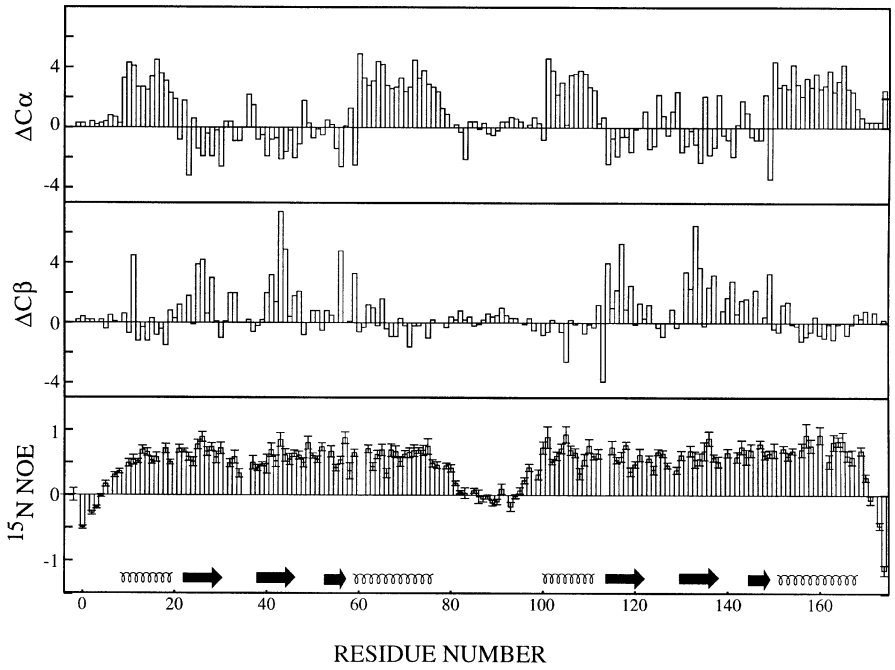


**Fig. 3.** Plots of $^{13}C_\alpha$ and $^{13}C_\beta$ secondary shifts and $^1H\{^{15}N\}$ heteronuclear NOEs versus dsRBD residue number. The extreme N- and C-terminal residues have strongly negative values, indicating that they are disordered in solution. The linker between the two dsRBMs shows much smaller NOEs, including some negative values, compared with ordered secondary structure regions, indicating that this region is highly flexible, consistent with its lack of long-range NOEs and scarce medium-range NOEs (see text).

Phe is bulky, which appears to preclude its binding into the narrow major groove. A substantial conformational change and widening of the RNA major groove would be required if its bases interact with dsRBM. On the other hand, the dsRBM-binding surface may cross over the major groove of the RNA duplex by hydrogen bonding

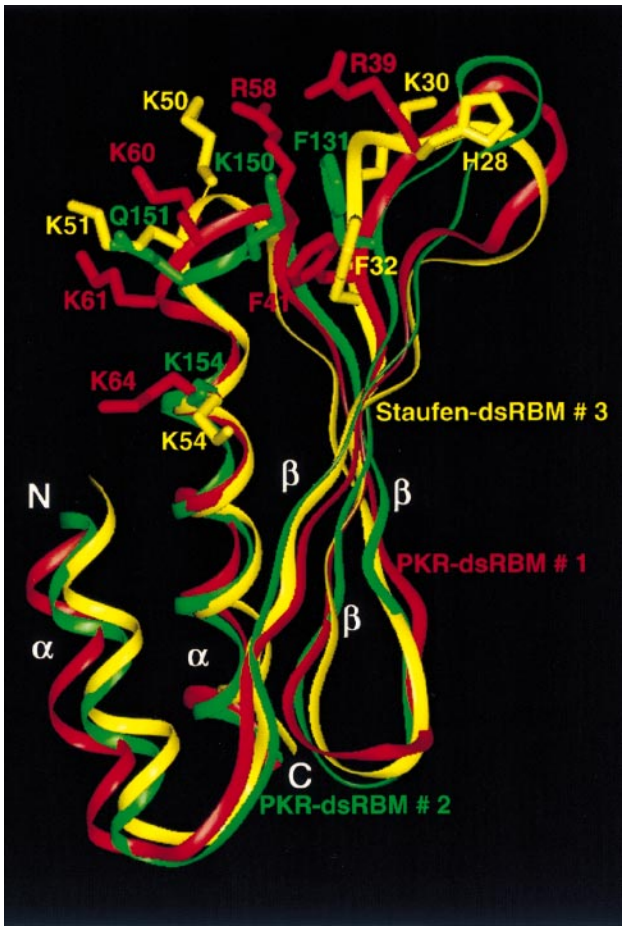


**Fig. 4.** Backbone superpositions of dsRBM1 (red) and dsRBM2 (green) for PKR, and dsRBM (yellow) for *Drosophila* Staufen protein (Bycroft *et al*., 1995), showing the similar fold of the motifs. The side chains of potential RNA-binding residues in each dsRBM are displayed, most of which are well conserved among dsRBMs. The *E.coli* RNA III dsRBM also has similar folding topology (Kharrat *et al*., 1995) but its PDB coordinates were not available in the PDB for detailed comparison.

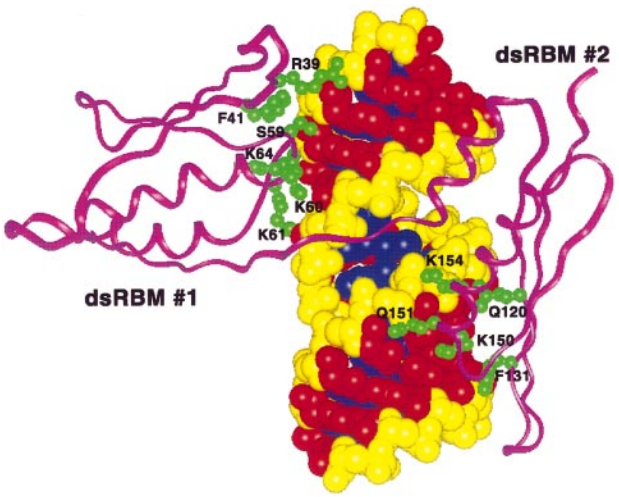


**Fig. 5.** Model of the interaction between the dsRBD and a 16 bp A form dsRNA helix. The model was built based on the following factors: (i) the RNA-binding sites are bulky and would bind to the minor groove without a substantial conformational change for the RNA duplex; (ii) dsRBD discriminates dsRNA over RNA–DNA and dsDNA, and specificity is due largely to molecular recognition of a network of 2′-OHs involving both strands of dsRNA (Bevilacqua and Cech, 1996); (iii) although dsRBD can bind as much as 30–33 bp if the linker is straight, the biochemical data have shown that dsRBD covers 11 bp. In this mode, only exposed side chains in the putative binding site on both dsRBM1 and dsRBM2 were docked onto the minor groove of the RNA duplex to form hydrogen bonds with the 2′-OHs on both strands. Several positively charged Lys side chains, including the conserved K64-$NH_3^+$ and K154-$NH_3^+$, not only hydrogen-bond with the 2′-OHs but also make the electrostatic interactions with the neighboring phosphate oxygens (–OP1, pointing out to surface). Because the linker is long and highly flexible, the two dsRBMs contact >8–11 bp by wrapping around the minor groove.

to the phosphate backbone; however, this possibility is eliminated since salt-dependent protein–RNA binding experiments revealed that 90% of the free energy of binding is non-electrostatic (Bevilacqua and Cech, 1996). In fact, detailed biochemical analyses have shown that the dsRBD of PKR exclusively binds dsRNA rather than RNA–DNA and dsDNA, and that this specificity is due mainly to recognition of a network of minor groove 2′-OHs and possibly some phosphate groups (Bevilacqua and Cech, 1996). This is consistent with our structural results in which the binding surface of each dsRBM seems to fit favorably into the wider minor groove by hydrogen bonding to 2′-OHs. A model for dsRBD–dsRNA interaction is presented in Figure 5, which combines both the structural and biochemical information. The model was built by docking the binding surfaces of the two dsRBMs onto a 16 bp A-form dsRNA derived from the HIV Tar that has been shown to bind PKR (Bevilacqua and Cech, 1996; B.W.Carpick and B.R.G.Williams, unpublished results). In the model, the binding surfaces in both motifs cover a total of 8–10 bp by wrapping around the minor groove of the RNA duplex, which agrees with the biochemical findings that the interactions occur along a 10–11 bp segment (Bevilacqua and Cech, 1996). Except for the non-polar interactions between the conserved Phe and the sugar, most of the hydrophilic residues in the RNA-binding sites favorably contact with 2′-OHs through hydrogen bonding. Interestingly, when docked to 2′-OHs for hydrogen bonding, some positively charged Lys side chains such as the conserved K64-$NH_3^+$ and K154-$NH_3^+$ groups are also within the distances to make electrostatic interactions with the negatively charged phosphate backbone oxygens (–OP1) that point out to the surface. This is possible because the salt-dependent dsRNA–dsRBD binding experiments have shown that ~10% of the free energy of binding is electrostatic involving the protein and dsRNA phosphate (Bevilacqua and Cech, 1996). Hence, this model helps to understand how dsRNA is recognized by dsRBD in a sequence-independent manner involving the minor groove 2′-OHs. Furthermore, the model indicates that the two flexibly linked dsRBMs can bind dsRNA in a coordinated fashion, leading to the rearrangement of the PKR conformation and its subsequent kinase activation (see below).

It is important to note here that numerous biochemical studies recently have suggested that dimerization is required for PKR activation (Patel *et al*., 1994, 1996; Cosentino *et al*., 1995; Romano *et al*., 1995; Wu and Kaufman, 1996, 1997). However, it remained elusive whether PKR dimerizes before or after dsRNA binding. We recently used four independent biophysical and biochemical approaches to investigate the PKR dimerization

and PKR–dsRNA interaction (Carpick *et al*., 1997). Neutron scattering data revealed that PKR is predominantly a dimer (high concentration), whereas the gel filtration analysis showed that PKR elutes predominantly as a monomer (low concentration), and addition of dsRNA significantly increased PKR dimerization (Carpick *et al*., 1997). Hence it was concluded that PKR exists in a monomer–dimer equilibrium in the absence of dsRNA and is sensitive to the protein concentration, and the dsRNA binding stabilizes the PKR dimerization in a 1:2 ratio (dsRNA:PKR) and causes a conformational change for kinase activation (Carpick *et al*., 1997). Our structural model (Figure 5) indicates that the two dsRBDs (four dsRBMs) could wrap around a longer dsRNA molecule side by side (preferably end to end), which would facilitate the PKR dimerization and the subsequent activation. While it was suggested that the dimerization may be mediated directly by dsRBD (Cosentino *et al*., 1995; Patel *et al*., 1995, 1996; Romano *et al*., 1995; Wu and Kaufman, 1996, 1997), a more recent study has shown that dimerization is mediated by the C-terminal region outside of the dsRBD (Tan *et al*., 1998). Indeed, the overall correlation time at high concentration (mM) and the gel filtration analysis at low concentration (μM) both indicated that dsRBD alone is in monomeric form (Nanduri *et al*., 1998), which is consistent with the dsRBM structures from *E.coli* RNase III and *Drosophila* Staufen protein also being monomeric (Bycroft *et al*., 1995; Kharrat *et al*., 1995). It should be pointed out, however, that dsRBD comprises only 31% of the total amino acids of full-length PKR, the entire structure of which remains unknown. It is possible that interdomain interactions within PKR play an important role in the regulation of kinase activity, and these interactions could be mediated through either the structured or unstructured regions of dsRBD or through both. It is also possible that dsRBD is partially involved in PKR dimerization and dsRBD alone is not able to form the stable dimer. The disparate results regarding PKR dimerization and the dimerization site may arise from differences in sample preparations including protein concentration, as mentioned above, buffer conditions, pH and other factors. For example, we have observed that bacterially overexpressed PKR and dsRBD, unless rigorously purified, can be contaminated by nucleic acids, and that dsRBD can self-associate through oxidation of cysteines (J.Qin *et al*., unpublished results).

It has long been established that PKR can be activated by low concentrations of dsRNA, while being inhibited by higher dsRNA concentrations (Williams *et al*., 1979). This appears explainable based on our structural model. While both dsRBMs are involved in dsRNA binding, the RNA-binding site in dsRBM2 appears less well conserved than that in dsRBM1 as compared with other dsRBMs (Figure 4), which is consistent with dsRBM2 having lower affinity than dsRBM1 (Green and Mathews, 1992; Schmedt *et al*., 1995). Hence, at lower dsRNA concentrations, the higher affinity dsRBM1 may first anchor to dsRNA and facilitate the cooperative dsRNA binding to lower affinity dsRBM2; however, once both dsRBMs are bound to dsRNA, addition of higher concentrations of dsRNA would no longer bind to PKR as shown before (Carpick *et al*., 1997), probably due to the saturation of the two RNA-binding sites in the wrap-around conformation. This is consistent with the finding that PKR, once activated, cannot be inhibited by subsequent addition of high concentrations of dsRNA (Galabru *et al*., 1989). On the other hand, if high dsRNA concentrations are added in the beginning, the binding may not be cooperative; for example, the two dsRBMs in PKR may simultaneously bind to two different dsRNA molecules, which leads to an unfavorable overall protein conformation for kinase activation. More detailed studies including the structures of PKR and the PKR–dsRNA complex will be necessary to define clearly the molecular mechanism of PKR activation.

## Materials and methods

### *NMR experiments*

The NMR sample preparation and the resonance assignments have been described previously (Nanduri *et al*., 1998), and the chemical shifts were deposited in BioMagResBank (accession No. BMRB4110). The dsRBD sample was prepared in argon-purged $H_2O$ solution (7% $^2H_2O$), 100 mM NaCl, 20 mM sodium phosphate pH 6.5 and 1 mM dithiothreitol (DTT) in a 250 μl microcell NMR tube (Shigemi Inc., Allison Park, PA) at a concentration of ~0.9 mM. All of the NMR experiments (Bax and Grzesiek, 1993; Canavagh *et al*., 1995; Kay, 1995) were conducted at 25°C using a Varian Inova 500 MHz spectrometer equipped with a triple resonance probe head and a shielded *z*-gradient unit. For structure determination, the following experiments were recorded on a 0.9 mM uniformly $^{15}$N-labeled protein and a 0.9 mM uniformly $^{15}$N/$^{13}$C-labeled protein, respectively: 3D water-flip-back $^{15}$N-separated NOESY, 3D $^{15}$N-separated HNHA, 3D $^{15}$N/$^{13}$C-edited NOESY, 4D $^{15}$N/$^{13}$C-edited NOESY and 4D $^{13}$C/$^{13}$C-edited NOESY. All the data were processed on a Sun UltraSPARC workstation using nmrPipe software (Delaglio *et al*., 1995). In the acquisition dimension, all data sets were processed identically. A solvent suppression filter was applied to the time domain data, followed by apodization with a 66° shifted squared-sine-bell window, zero-filling to the next power of 2, Fourier transformation and phasing. The data were apodized in t2 by a 72° shifted sine-bell window prior to zero-filling to 256 complex points, Fourier transformation and phasing. The processed spectra were analyzed by the PIPP program (Garrett *et al*., 1991).

### *Structure calculations*

The structure of dsRBD was calculated on a SGI Indigo2 R10000 workstation using a modified protocol (Nilges *et al*., 1988), which makes use of the program X-PLOR (version 3.2) (Brünger, 1993). The target function that is minimized during simulated annealing (SA) is comprised of quadratic harmonic potential terms for covalent geometry, square-well quadratic potentials for the experimental distance and torsion angle restraints, harmonic potentials for the $^3J_{HNHA}$ coupling constant (Garrett *et al*., 1994), and $^{13}C_\alpha$ and $^{13}C_\beta$ secondary chemical shifts (Kuszewski *et al*., 1995) and a quadratic van der Waals repulsion term for the non-bonded contacts. No hydrogen bonding, electrostatic or 6–12 Lennard–Jones empirical potential energy terms were included in the target function. Hydrogen bonding restraints, which account for the slowly exchanging backbone amide protons in regular secondary structure regions, were only included in the calculation during the final stage of refinement. A total of 3215 experimental restraints were used in the structure calculation. These include 2580 NOE distance restraints, 146 hydrogen bond restraints, 137 $\phi$, 27 $\chi_1$ derived from 33 stereospecific assignments, 139 $^3J_{HNHA}$ values, 175 $C_\alpha$ and 157 $C_\beta$ shifts. The distance restraints were grouped into four distance ranges, 1.8–2.5 , 1.8–3.5, 1.8–5.0 and 1.8–6.0 Å, corresponding to strong, medium, weak and very weak NOEs. $\phi$ and $\chi_1$ were derived from the coupling constants and NOE data, and the minimum ranges employed were $\pm$15° and $\pm$20° respectively (Nilges *et al*., 1990). Thirty final SA structures were generated, and the detailed statistics are shown in Table I.

## Acknowledgements

We thank Frank Delaglio and Dan Garrett for nmrPipe and Pipp software. The work was supported in parts by grants from the American Heart Association and Ohio regents of board to J.Q., and NIH R01AI34039 to B.R.W.

## References


Bax,A. and Grzesiek,S. (1993) Methodological advances in protein NMR. *Acc. Chem. Res.*, **26**, 131–138.

Beretta,L., Gabbay,M., Berger,R., Hanash,S.M. and Sonenberg,N. (1996) Expression of the protein kinase PKR is modulated by IRF-1 and is reduced in 5q-associated leukemias. *Oncogene*, **12**, 1593–1596.

Bevilacqua,P.C. and Cech,T.R. (1996) Minor-groove recognition of double-stranded RNA by the double-stranded RNA-binding domain from the RNA-activated protein kinase PKR. *Biochemistry*, **35**, 9983–9994.

Brand,S.R., Kobayashi,R. and Mathews,M.B. (1997) The Tat protein of human immunodeficiency virus type 1 is a substrate and inhibitor of the interferon-induced, virally activated protein kinase, PKR. *J. Biol. Chem.*, **272**, 8388–8395.

Brünger,A.T. (1993) *XPLOR Version 3.1 Manual*. Yale University Press, New Haven, CT.

Bycroft,M., Grunert,S., Murzin,A.G., Proctor,M. and St Johnston,D. (1995) NMR solution structure of a dsRNA binding domain from *Drosophila* staufen protein reveals homology to the N-terminal domain of ribosomal protein S5. *EMBO J.*, **14**, 3563–3571.

Canavagh,J., Fairbrother,W.J., Palmer,A.G. and Skelton,N.J. (1995) *Protein NMR Spectroscopy*. Academic Press, San Diego, CA.

Carpick,B.W., Graziano,V., Schneider,D., Maitra,R.K., Lee,K. and Williams,B.R.G. (1997) Characterization of the solution complex between the interferon-induced, double-stranded RNA-activated protein kinase and HIV-1 TAR RNA. *J. Biol. Chem.*, **272**, 9510–9516.

Chong,K.L., Feng,L., Schappert,K., Meurs,E., Donahue,T.F., Friesen,J.D., Hovanessian,A.G. and Williams,B.R.G. (1992) Human p68 kinase exhibits growth suppression in yeast and homology to the translational regulator GCN2. *EMBO J.*, **11**, 1553–1562.

Clarke,P.A. and Mathews,M.B. (1995) Interactions between the double-stranded RNA binding motif and RNA: definition of the binding site for the interferon-induced protein kinase DAI (PKR) on adenovirus VA RNA. *RNA*, **1**, 7–20.

Clemens,M.J. (1997) PKR—a protein kinase regulated by double-stranded RNA. *Int. J. Biochem. Cell. Biol.*, **29**, 945–949.

Cosentino,G.P., Venkatesan,S., Serluca,F.C., Green,S.R., Mathews,M.B. and Sonenberg,N. (1995) Double-stranded-RNA-dependent protein kinase and TAR RNA-binding protein form homo- and heterodimers *in vivo*. *Proc. Natl Acad. Sci. USA*, **92**, 9445–9449.

Delaglio,F., Grzesiek,S., Vuister,G.W., Zhu,G., Pfeifer,J. and Bax,A. (1995) NMRPipe: a multidimensional spectral processing system based on UNIX PIPES. *J. Biol. NMR*, **6**, 277–293.

Der,S.D., Yang,Y.L., Weissmann,C. and Williams,B.R.G. (1997) A double-stranded RNA-activated protein kinase-dependent pathway mediating stress-induced apoptosis. *Proc. Natl Acad. Sci. USA*, **94**, 3279–3283.

Donze,O., Jagus,R., Koromilas,A.E., Hershey,J.W. and Sonenberg,N. (1995) Abrogation of translation initiation factor eIF-2 phosphorylation causes malignant transformation of NIH 3T3 cells. *EMBO J.*, **14**, 3828–3834.

Galabru,J. and Hovanessian,A.G. (1985) Two interferon-induced proteins are involved in the protein kinase complex dependent on double-stranded RNA. *Cell*, **43**, 685–694.

Galabru,J., Katze,M.G., Robert,N. and Hovanessian,A.G. (1989) The binding of double-stranded RNA and adenovirus VAI RNA to the interferon-induced protein kinase. *Eur. J. Biochem.*, **178**, 581–589.

Garrett,D.S., Powers,R., Gronenborn,A.M. and Clore,G.M. (1991) A common sense approach to eak picking in two- three- and four-dimensional spectra using automatic computer analysis of contour diagrams. *J. Magn. Reson.*, **95**, 214–220.

Garrett,D.S., Kuszewski,J., Hancock,T.J., Lodi,P.J., Vuister,G.W., Gronenborn,A.M. and Clore,G.M. (1994) The impact of direct refinement against three-bond HN-$C^{\alpha}H$ coupling constants on protein structure determination by NMR. *J. Magn. Reson.*, **B104**, 99–103.

Green,S.R. and Mathews,M.B. (1992) Two RNA-binding motifs in the double-stranded RNA-activated protein kinase, DAI. *Genes Dev.*, **6**, 2478–2490.

Hunter,T., Hunt,T., Jackson,R.J. and Robertson,H.D. (1975) The characteristics of inhibition of protein synthesis by double-stranded ribonucleic acid in reticulocyte lysates. *J. Biol. Chem.*, **250**, 409–417.

Kay,L.E. (1995) Field gradient techniques in NMR spectroscopy. *Curr. Opin. Struct. Biol.*, **5**, 674–681.

Kharrat,A., Macias,M.J., Gibson,T.J., Nilges,M. and Pastore, A. (1995) Structure of the dsRNA binding domain of *E.coli* RNase III. *EMBO J.*, **14**, 3572–3584.

Koromilas,A.E., Roy,S., Barber,G.N., Katze,M.G. and Sonenberg,N. (1992) Malignant transformation by a mutant of the IFN-inducible dsRNA-dependent protein kinase. *Science*, **257**, 1685–1689.

Kraulis,P.J. (1991) MOLSCRIPT—a program to produce both detailed and schematic plots of protein structures. *J. Appl. Crystallogr.*, **24**, 946–950.

Kumar,A., Haque,J., Lacoste,J., Hiscott,J. and Williams,B.R.G. (1994) Double-stranded RNA-dependent protein kinase activates transcription factor NF-κB by phosphorylating I kappa B. *Proc. Natl Acad. Sci. USA*, **91**, 6288–6292.

Kumar,A., Yang,Y.L., Flati,V., Der,S., Kadereit,S., Deb,A., Haque,J., Reis,L., Weissmann,C. and Williams,B.R.G. (1997) Deficient cytokine signaling in mouse embryo fibroblasts with a targeted deletion in the PKR gene: role of IRF-1 and NF-kappaB. *EMBO J.*, **16**, 406–416.

Kuszewski,J., Qin,J., Gronenborn,A.M. and Clore,G.M. (1995) The impact of direct refinement against $^{13}C_{\alpha}$ and $^{13}C_{\beta}$ chemical shifts on protein structure determination by NMR. *J. Magn. Reson.*, **B106**, 92–96.

Manche,L., Green,S.R., Schmedt,C. and Mathews,M.B. (1992) Interactions between double-stranded RNA regulators and the protein kinase DAI. *Mol. Cell. Biol.*, **12**, 5238–5248.

Maran,A., Maitra,R.K., Kumar,A., Dong,B., Xiao,W., Li,G., Williams,B.R.G., Torrence,P.F. and Silverman,R.H. (1994) Blockage of NF-kappa B signaling by selective ablation of an mRNA target by 2–5A antisense chimeras. *Science*, **265**, 789–792.

McMillan,N.A., Carpick,B.W., Hollis,B., Toone,W.M., Zamanian-Daryoush,M. and Williams,B.R.G. (1995) Mutational analysis of the double-stranded RNA (dsRNA) binding domain of the dsRNA-activated protein kinase, PKR. *J. Biol. Chem.*, **270**, 2601–2606.

Meurs,E., Chong,K., Galabru,J., Thomas,N.S., Kerr,I.M., Williams,B.R.G. and Hovanessian,A.G. (1990) Molecular cloning and characterization of the human double-stranded RNA-activated protein kinase induced by interferon. *Cell*, **62**, 379–390.

Minks,M.A., West,D.K., Benvin,S. and Baglioni,C. (1979) Structural requirements of double-stranded RNA for the activation of 2′,5′-oligo(A) polymerase and protein kinase of interferon-treated HeLa cells. *J. Biol. Chem.*, **254**, 10180–10183.

Nanduri,S., Carpick,B.W., Yang,Y., Williams,B.R.G. and Qin,J. (1998) $^{1}H$, $^{13}C$, $^{15}N$ resonance assignment of the 20 kDa dsRNA binding domain of protein kinase PKR. *J. Biomol. NMR*, in press.

Nilges,M., Clore,G.M. and Gronenborn,A.M. (1988) Determination of three-dimensional structures of proteins from interproton distance data by hybrid distance geometry–dynamical simulated annealing calculations. *FEBS Lett.*, **229**, 317–324.

Nilges,M., Clore,G.M. and Gronenborn,A.M. (1990) $^{1}H$-NMR stereospecific assignments by conformational data-base searches. *Biopolymers*, **29**, 813–822.

Palvetich,N.P. and Pabo,C.O. (1991) Zinc-finger-DNA recognition: crystal structure of a Zif268–DNA complex at 2.1 Å. *Science*, **252**, 809–817.

Patel,R.C. and Sen,G.C. (1992) Identification of the double-stranded RNA-binding domain of the human interferon-inducible protein kinase. *J. Biol. Chem.*, **267**, 7671–7676.

Patel,R.C., Stanton,P. and Sen,G.C. (1994) Role of the amino-terminal residues of the interferon-induced protein kinase in its activation by double-stranded RNA and heparin. *J. Biol. Chem.*, **269**, 18593–18598.

Patel,R.C., Stanton,P., McMillan,N.M., Williams,B.R.G. and Sen,G.C. (1995) The interferon-inducible double-stranded RNA-activated protein kinase self-associates *in vitro* and *in vivo*. *Proc. Natl Acad. Sci. USA*, **92**, 8283–8237.

Patel,R.C., Stanton,P. and Sen,G.C. (1996) Specific mutations near the amino terminus of double-stranded RNA-dependent protein kinase (PKR) differentially affect its double-stranded RNA binding and dimerization properties. *J. Biol. Chem.*, **271**, 25657–25663.

Rice,A.P., Duncan,R., Hershey,J.W. and Kerr,I.M. (1985) Double-stranded RNA-dependent protein kinase and 2–5A system are both activated in interferon-treated, encephalomyocarditis virus-infected HeLa cells. *J. Virol.*, **54**, 894–898.

Romano,P.R., Green,S.R., Barber,G.N., Mathews,M.B. and Hinnebusch, A.G. (1995) Structural requirements for double-stranded RNA binding, dimerization, and activation of the human eIF-2 alpha kinase DAI in *Saccharomyces cerevisiae*. *Mol. Cell. Biol.*, **15**, 365–378.

Samuel,C.E., Duncan,R., Knutson,G.S. and Hershey,J.W. (1984) Mechanism of interferon action. Increased phosphorylation of protein synthesis initiation factor eIF-2 alpha in interferon-treated, reovirus-infected mouse L929 fibroblasts *in vitro* and *in vivo*. *J. Biol. Chem.*, **259**, 13451–13457.

Schmedt,C., Green,S.R., Manche,L., Taylor,D.R., Ma,Y. and Mathews, M.B. (1995) Functional characterization of the RNA-binding domain and motif of the double-stranded RNA-dependent protein kinase DAI (PKR). *J. Mol. Biol.*, **249**, 29–44.

Tan,S.-L., Gale,M.J.,Jr and Katze,M.G. (1998) Double-stranded RNA-independent dimerization of interferon-induced protein kinase PKR and inhibition of dimerization by the cellular P581PK inhibitor. *Mol. Cell. Biol.*, **18**, 2431–2443.

Williams,B.R.G. (1995) The role of the dsRNA-activated kinase, PKR, in signal transduction. *Semin. Virol.*, **6**, 191–202.

Williams,B.R.G., Gilbert,C.S. and Kerr,I.M. (1979) The respective roles of the protein kinase and pppA2′ p5′ A2′ p5 A-activated endonuclease in the inhibition of protein synthesis by double stranded RNA in rabbit reticulocyte lysates. *Nucleic Acids Res.*, **6**, 1335–1350.

Wong,A.H., Tam,N.W., Yang,Y.L, Cuddihy,A.R., Li,S., Kirchhoff,S., Hauser,H., Decker,T. and Koromilas,A.E. (1997) Physical association between STAT1 and the interferon-inducible protein kinase PKR and implications for interferon and double-stranded RNA signaling pathways. *EMBO J.*, **16**, 1291–1304.

Wu,S. and Kaufman,R.J. (1996) Double-stranded (ds) RNA binding and not dimerization correlates with the activation of the dsRNA-dependent protein kinase (PKR). *J. Biol. Chem.*, **271**, 1756–1763.

Wu,S. and Kaufman,R.J. (1997) A model for the double-stranded RNA (dsRNA)-dependent dimerization and activation of the dsRNA-activated protein kinase PKR. *J. Biol. Chem.*, **272**, 1291–1296.

Zhu,S., Romano,P.R. and Wek,R.C. (1997) Ribosome targeting of PKR is mediated by two double-stranded RNA-binding domains and facilitates *in vivo* phosphorylation of eukaryotic initiation factor-2. *J. Biol. Chem.*, **272**, 14434–14441.

*Received June 17, 1998; revised and accepted July 20, 1998*